Transferred hyperfine interaction and structure in $LiMn_2O_4$ and Li_2MnO_3 coexisting phases: A XRD and ^{7}Li NMR-MAS study

Piercarlo Mustarelli, Vincenzo Massarotti, Marcella Bini, and Doretta Capsoni
CSTE-CNR and Department of Physical Chemistry, University of Pavia, Via Taramelli 16, 27100 Pavia, Italy
(Received 30 September 1996)

X-ray diffraction (XRD) and ^{7}Li NMR-MAS measurements have been performed on $LiMn_2O_4$ (lithium cationic fraction, $x=0.333$), Li_2MnO_3 ($x=0.667$), and the intermediate composition with $x=0.40$. The use of magic angle spinning produces complex manifolds of the spinning sidebands. The predominant interaction affecting the NMR spectrum is the transferred hyperfine coupling (TFHI) between the Mn ions and the Li spins. TFHI parameters are extracted from MAS-NMR spectra of oxides containing a large quantity of manganese. We obtained a full spectral assignment for the spinel $LiMn_2O_4$, for the rocksalt Li_2MnO_3, and for the $x=0.40$ sample, which contains the rocksalt and both stoichiometric and nonstoichiometric spinel phases. According to XRD data, the rocksalt phase contains three nonequivalent lithium sites whose NMR peaks are shifted upfield from $x=0.667$ to 0.40 because of the cell volume expansion. The Li^+ ions belonging to the two spinel phases of $x=0.40$ are quite mobile and give origin by motional narrowing to a single peak, which is slightly shifted upfield with respect to that of $LiMn_2O_4$. [S0163-1829(97)01814-6]

I. INTRODUCTION

Li-Mn-O compounds have recently gained a great deal of attention since the $LiMn_2O_4$ spinel and related phases possess peculiar transport properties, and capabilities of lithium intercalation/deintercalation, which allow applications in electrochemistry[1] and catalysis.[2,3] We have recently studied by x-ray diffraction the formation of $LiMn_2O_4$ from the reactive system MnO/Li_2CO_3.[4] We characterized a monophasic region (Li cationic fraction $0.333<x\leqslant 0.35$) in which the spinel compound is stable, and a second one ($0.36\leqslant x<0.667$) where two spinels (stoichiometric, phase I, and nonstoichiometric, phase II) and Li_2MnO_3 coexist.

The stoichiometry of $LiMn_2O_4$ ($x=0.333$) and Li_2MnO_3 ($x=0.667$) coexisting phases and their abundance were addressed by electron-paramagnetic-resonance (EPR) and x-ray-diffraction (XRD) measurements.[5] The structures of the two compounds are known.[6,7] We showed that structural defects and stoichiometry of the phases can depend on the preparation conditions.

The peculiar physicochemical properties of the transition-metal compounds are due to the coupling of the cation electronic structure with the local crystal field. Nuclear magnetic resonance may give valuable hints in understanding the relationships among structure, covalency, defects and conductivity. ^{7}Li solid-state NMR was early employed to investigate magnetic order and superexchange interactions in $LiMnPO_4$.[8] Shulman and Jaccarino used ^{19}F NMR to study the relationships between covalency and long-range order in paramagnetic MnF_2.[9] Shulman and Knox obtained the isotropic and anisotropic hyperfine interactions in $KMnF_3$.[10]

More recently, NMR with magic angle spinning (MAS) has been shown to be useful in studies of paramagnetic solids.[11] Rothwell *et al.* reported, for a natural mineral, the occurrence of spinning sidebands markedly enhanced relative to those of the corresponding diamagnetic synthetic compound, presumably as a result of para- or ferromagnetic impurities.[12] Olejniczak *et al.* gave a general approach to analyze combined MAS−multiple-pulse experiments.[13] Nayeem and Yesinowski provided a quantitative interpretation of the intensity pattern of the spinning sidebands in paramagnetic solids, which is due to inhomogeneous interactions.[14] Enhanced sideband intensities and substantial isotropic paramagnetic shifts have been observed by ^{119}Sn NMR-MAS in rare-earth stannates.[15,16]

Transition metals as well as other metals oxides have been studied by ^{7}Li NMR-MAS. Dalton *et al.* resolved tetrahedral and octahedral Li sites in the superconducting spinel $Li_{1+y}Ti_{2-y}O_4$ for $y>0$.[17] Ganguly *et al.* found large shifts and broad linewidths in $LiNiO_2$. They argued that the substitution of Ni by Li in NiO creates holes on Ni.[18] The substitution of Ni by Co in the solid solution $LiNi_{1-y}Co_yO_2$ has been recently studied by ^{6}Li and ^{7}Li NMR.[19]

The system Li/Mn/O has only recently been studied by NMR. Kanzaki *et al.*[20] presented some shift values for $LiMn_2O_4$ and Li_2MnO_3, that they attributed to the Knight shift. On this basis, they attributed to lithium a ''density of state'' ~ 1 in $LiMn_2O_4$ which, however, has been told to display a high electric resistance. Kumagai *et al.*[21] also assigned to $LiMn_2O_4$ a metallic character which, however, is in disagreement with their own XRD and XPS results. Finally, Morgan *et al.*[22] studied both $LiMn_2O_4$ and Li_2MnO_3 by ^{6}Li and ^{7}Li NMR. However, some of their results suggest a partially incorrect determination of the isotropic chemical shifts. The magnetic properties of $LiMn_2O_4$ have been recently investigated by Masquelier *et al.*[23]

In this paper we perform a careful XRD and ^{7}Li NMR-MAS analysis of the two cited compounds and of an intermediate composition ($x=0.4$). We are able to assign the observed peaks to magnetically nonequivalent lithium ions. The shifts are interpreted in terms of transferred hyperfine interaction (TFHI) between the Mn ions and the lithium nuclear spins. The values of the TFHI constant are deduced for the different cases.

II. EXPERIMENT

A. Sample preparation

The samples were prepared by the reactive system Alfa (99.9%) MnO/Carlo Erba (R.P.) Li_2CO_3 from starting mixture having $x=0.333$, 0.40, and 0.667. Each mixture was fired in air 8 h at 900 °C. For $x=0.333$ an additional treatment of 1 h at 1100 °C was performed. Both heating and cooling rates were 5 °C min. Several other samples were prepared in the range $0.333 \leqslant x \leqslant 0.53$, and investigated only by XRD.

B. NMR measurements

The NMR measurements were performed on a AMX400WB spectrometer (Bruker, Karlsruhe, Germany) with a 9.4-T magnet. ^{7}Li nucleus resonates at 155.6 MHz. Both static and MAS measurements were performed with a 4 mm CP-MAS probe (Bruker). Spinning speeds from 6 to 13 kHz were employed. A single-pulse sequence was used with a pulse width of 0.5 μs, corresponding to a tip angle of $\sim 30°$. The FID's were left-shifted and Fourier transformed without line broadening. The spectra were referenced to an external sample of 1.0 M LiCl in H_2O.

The obtained spectra consist of complex spinning-sideband manifolds. In the case of Li_2MnO_3, for example, the manifold spans over several thousands ppm. Except for the spinel composition, we met with severe difficulties in finding isotropic chemical shifts. The problems were mainly due (i) to the overlapping of the spinning sidebands with the isotropic resonances and, (ii) to the uncertainties in phasing the spectra. To overcome these problems we performed our experiments at several MAS speeds, and each spectrum was phased following different criteria. Each spectrum belonging to the matrix (speed×phasing) was then compared with the others and the best isotropic candidates were extracted on the basis of their statistical occurrence. In the case of Li_2MnO_3 we obtained a good agreement with the results of Ref. 22.

We also tried to use a spin-echo sequence with the echo delay time synchronized with the rotor period.[14,15] However, no significant improvements were obtained concerning the phasing procedure.

C. XRD measurements

Diffraction data were obtained by a Philips PW 1710 powder diffractometer equipped with a Philips PW 1050 vertical goniometer. Use was made of the Cu $K\alpha$ radiation ($K\alpha_1=1.5406$ Å; $K\alpha_2=1.5443$ Å) obtained by means of a graphite monochromator. Patterns were collected in the angular range $15°<2\theta<130°$ in a step scan mode (step width 0.02° and 0.025°, counting time 10 s).

Structural and profile parameters were obtained by the Rietveld profile refinement (RPR) procedure.[24] The refinement was performed with the programs DBWS (Ref. 25) and WYRIET version 3.5.[26] More detailed descriptions about Rietveld refinement of multiphase systems has been reported in previous papers.[4,27] The structural model to fit the observed patterns depends on the mixture composition, which determines the presence and abundance of the stoichiometric and nonstoichiometric spinel and of Li_2MnO_3 phases. The multiphase refinement of several samples in the range $0.333 \leqslant x \leqslant 0.53$ was performed to determine the x dependence of the lattice parameters of the coexisting compounds.

III. THEORETICAL BACKGROUND

Magnetic materials are characterized by the presence of unpaired electron spins which arise from d or f electrons in unfilled shells of atoms or ions. The effective field, and then the NMR shift, will be changed by an amount that depends on the quantity and state of unpaired electrons at the ion site, and on the hyperfine interaction of the electrons with the nucleus.

Generally speaking, three sources contribute to the hyperfine field: the local one, the core one, and the field due to conduction electrons.[28] In insulating materials only the first two terms contribute the interaction. The Hamiltonian of the hyperfine interaction in its more general form is

$$H_N = -g g_I \beta \beta_N \left\{ \frac{8\pi}{3}\,\delta(\mathbf{r})(\mathbf{I}\cdot\mathbf{S}) + \frac{(\mathbf{L}-\mathbf{S})\cdot I}{r^3} + \frac{3(\mathbf{S}\cdot\mathbf{r})(\mathbf{I}\cdot\mathbf{r})}{r^5} \right\}, \tag{1}$$

where **L**, **S**, and **I** are electron orbital, electron spin, and nuclear spin operators, respectively, r is the distance measured from the center of the nucleus, and the other symbols have the usual meaning. The first addendum in the brackets is the Fermi contact term, and the last two terms represent the dipolar interactions between the nuclear spin and the electron angular and spin momenta, respectively. If the orbital angular momentum is totally quenched the second term may be neglected.

The expectation value of $\mathbf{H}_N$ over the orbital part $|\phi\rangle$ of the total wave function is a second-rank tensor **F** which couples **I** and **S**. This tensor can be split into a traceless part $\mathbf{F}_1$ and a diagonal part $\mathbf{F}_2$. The isotropic part of $|\phi\rangle$ contributes the term

$$\mathbf{I}\cdot\mathbf{F}_2\cdot\mathbf{S} = -\frac{16}{3}\,\pi\beta\gamma\sum_n a_n a_n^* \langle \phi_n | \delta(\mathbf{r})\mathbf{S}\cdot\mathbf{I} | \phi_n \rangle, \tag{2}$$

where

$$\mathbf{F}_2 = A = -\frac{16}{3}\,\pi\beta\gamma\sum_n |a_n|^2 |\phi_n(0)|^2 \tag{3}$$

and A is familiar as the hyperfine interaction tensor. If we neglect the electron spin-orbit coupling, the off-diagonal elements of the orthonormal expansion of $|\phi\rangle$ give the dipolar term

$$\mathbf{I}\cdot\mathbf{F}_1\cdot\mathbf{S} = -2\beta\gamma\sum_l \sum_{l'} a_l a_{l'}^* \times \left\langle \phi_{l'} \left| \frac{3(\mathbf{I}\cdot\mathbf{r})(\mathbf{S}\cdot\mathbf{r})}{r^5} - \frac{\mathbf{I}\cdot\mathbf{S}}{r^3} \right| \phi_l \right\rangle. \tag{4}$$

In the case of interaction among a nucleus and electrons of different atoms, the coupling, C, for each electron is given by

$$C=\frac{16}{3}\hbar\pi\gamma\beta(\mathbf{I}\cdot\mathbf{S})|\phi(\mathbf{R})|^2+2\hbar\beta\gamma I \times \mathrm{grad}_{\mathbf{R}}\int \frac{\mathrm{div}(S\rho(r))}{|\mathbf{r}-\mathbf{R}|}\,d^3r, \quad (5)$$

where $\rho(r)=|\phi(r)|^2$ and $\mathbf{R}$ is the distance from the nuclear spin to the atoms. The first term is the Fermi contact, and the second is the dipolar one, which may have both isotropic and anisotropic contributions. Only the anisotropic part is removed (or reduced) by MAS. The peak's isotropic shift arises both from the Fermi contact term [$|\phi(0)|^2\neq 0$ at the nuclear position], and from the pseudocontact one. This last term is given by the combined effects of (nuclear spin-electron spin) and (electron orbit-nuclear spin) dipolar coupling, and is nonzero only for systems where the electron tensor g is anisotropic. The pseudocontact shift, δ_p, in a polycrystalline solid has been derived in the high-temperature limit by McConnell and Robertson[29]

$$\delta_p=-(3\cos^2\varsigma-1)(g_{\mathrm{par}}^2-g_{\mathrm{perp}}^2)\beta^2H_0S(S+1)/9kTR^3, \quad (6)$$

where g_{par} and g_{perp} are the splitting factors parallel and perpendicular to the symmetry axis, respectively. The Fermi contact Hamiltonian can be expressed in terms of the hyperfine coupling constant, A,

$$H_N=\hbar AS_zI_{Nz}. \quad (7)$$

In a system characterized by an electron relaxation time $T_e^{-1}\gg A$, the nucleus will see an average hyperfine magnetic field that will give a total shift

$$\Delta\omega=\gamma_NH_0-\frac{A}{h}\langle S_z\rangle, \quad (8)$$

where the sign of A will give the direction of the shift. The time-averaged value of the electron spin in the high-temperature approximation is given by

$$\langle S_z\rangle=-g|\beta|\frac{S(S+1)H_0}{3kT}. \quad (9)$$

The hyperfine interaction due to many magnetic ions may be considered as additive, so the total shift will be

$$\Delta\omega=\sum_i\frac{A_i}{h}\langle S_z\rangle. \quad (10)$$

It is interesting to make some considerations about the observability of the NMR signal. Due to the large electronic magnetic field at the nucleus site, the Zeeman term may no longer be the dominant one in the Hamiltonian. Further, the strong hyperfine interaction between electrons and nucleus enhances the relaxation processes and broadens the NMR line.

The concentration of magnetic ions plays a positive role in making the NMR signal more detectable. In fact, the exchange interaction among electron spins provides for fast spin flipping, which results in a much attenuated electronic dipolar field seen by the nucleus. For strong exchange couplings of the form $\hbar\nu S_1\cdot S_1$ between neighboring electron spins, a flip-flop process involving the electrons occurs at a frequency $\nu\sim 1/\tau$. The nucleus ''sees'' an electronic field fluctuating at a frequency ν and the NMR signal is observable if the conditions $A\tau\cong 1$ and $A^2\tau\ll\gamma H_0$ are fulfilled.

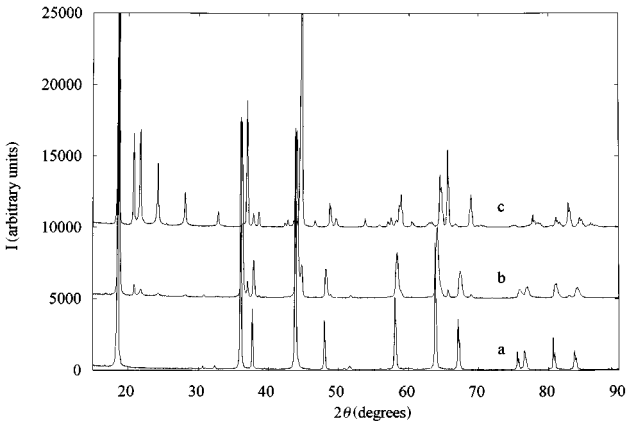

FIG. 1. XRD patterns for the samples $x=0.333$ (a), $x=0.40$ (b), and $x=0.667$ (c).

IV. RESULTS AND DISCUSSION

A. The XRD information

The sample patterns were characterized by the lines expected for the spinel phase for x values near 0.333 [Fig. 1(a)], or by those expected for the Li_2MnO_3 phase for $x\cong 0.667$ [Fig. 1(c)]. For the intermediate composition $x=0.40$ both line sets were observed [Fig. 1(b)] and the structural parameters refinement for multiphase system was performed, taking into account also the presence of a Li-rich spinel phase in addition to the stoichiometric spinel.[4,5]

From the RPR analysis, the abundance and the stoichiometry of the phases and the values of cell parameters were determined according to the procedure reported in Ref. 4. Figure 2 shows the values of cell volumes for the spinels [Figs. 2(a) and 2(b)] and for Li_2MnO_3 [Fig. 2(c)] as a function of x. Both the stoichiometric [Fig. 2(a)] and the Li-rich

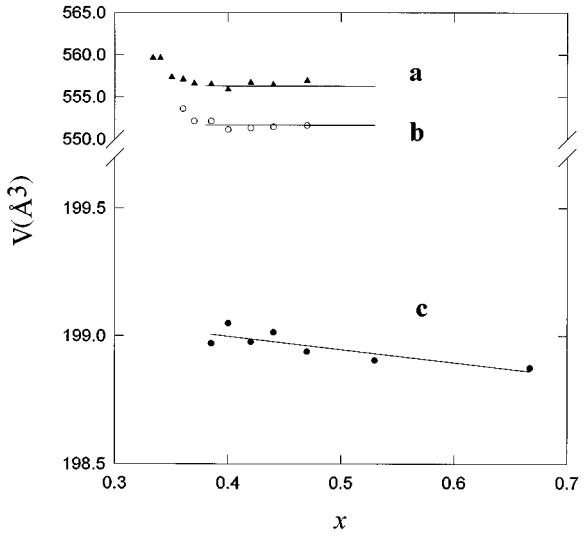

FIG. 2. Cell volumes as a function of x for (a) stoichiometric spinel, (b) nonstoichiometric spinel, and (c) Li_2MnO_3. The lines are a guide to the eye.

TABLE I. The Li-Mn average distances are calculated over all manganese belonging to the first shell of each lithium. *, Li-Mn distances through vertices (see text); +, $Li_{octahetral}$-Mn distances.

Samples	Phase	$\langle S_z \rangle$	A/h (cm^{-1})	Shift (ppm)	Li-Mn (Å)
$x=0.333$	Spinel (stoich.)	0.575	0.38×10^{-4}	664	12×3.417
	Spinel (stoich.)	0.575	0.38×10^{-4}	658	12×3.410
	Spinel (nonstoich.)	0.575	0.38×10^{-4}	658	12×3.401
					12×2.916+
$x=0.40$	Rocksalt (Li1)	0.4	1.30×10^{-4}	1600	6×2.842
	Rocksalt (Li2)	0.4	0.69×10^{-4}	848	4×2.890
					4×4.042*
	Rocksalt (Li3)	0.4	0.64×10^{-4}	787	4×2.895
					4×4.035*
$x=0.667$	Rocksalt (Li1)	0.4	1.44×10^{-4}	1770	6×2.842
	Rocksalt (Li2)	0.4	0.71×10^{-4}	875	4×2.888
					4×4.039*
	Rocksalt (Li3)	0.4	0.69×10^{-4}	850	4×2.893
					4×4.034*

[Fig. 2(b)] spinel undergo a decrease of the cell volume for $x \leqslant 0.40$, whereas for $x > 0.40$ the volumes remain nearly constant. This result agrees with the fact that a limiting composition is reached for both spinel phases.[5] Figure 2(c) shows a slight decrease in the range $0.38 \leqslant x \leqslant 0.667$.

The RPR method allows one to know the coordinates of the neighboring cations of lithium atoms. The number and position of the Mn atoms neighboring to the lithium sites allow one to estimate the Li-Mn interactions that dominate the NMR spectra.

$LiMn_2O_4$ (phase I). The lithium atoms occupy the tetrahedral sites of the structure. There are 12 neighboring octahedral Mn^{3+} and Mn^{4+}. The distances Li-Mn are reported in Table I. As no inversion is found, only one type of lithium site is present in the structure of the stoichiometric spinel.

$Li[Li_yMn_{2-y}]O_4$ (phase II). In addition to the already described tetrahedral lithium, the presence of some lithium on the octahedral site has been determined by Rietveld analysis. The value of y is well known as a function of the initial composition[5] and is about 0.2 for the samples with $x=0.40$, that means about 10% of lithium ions on the octahedral sites. The distances between Mn atoms and both regular and substitutional lithium are reported in Table I.

Li_2MnO_3. The three crystallographically independent lithium sites in the monoclinic structure (space group $C2/m$) can be described in the following fashion.

Li1. It is at the center of oxygen octahedra slightly distorted with four Li-O distances of 2.055 Å and two of 2.071 Å. The octahedron is connected through the vertices with 6 octahedra centered on lithium atoms and shares edges with 12 other octahedra, 6 of which are centered on Mn. Figure 3 shows the spatial arrangement of the 6 Mn^{4+} ions surrounding the Li1 site. The Li-Mn distances range between 2.837 and 2.844 Å and their average value is reported in Table I.

Li2. It is at the center of oxygen octahedra with four long distances (2.147 Å) and two short ones (2.009 Å). This octahedron is connected through the vertices with 6 octahedra, 4 of which with Mn at the center, and through the edges with 12 octahedra, 4 of which with central Mn. The average values are reported in Table I. Figure 4 shows the spatial arrangement of the 8 Mn polyhedra surrounding the Li2 site.

Li3. It is the central ion of oxygen octahedra with two distances of 2.167 Å, two of 2.098 Å, and two of 2.043 Å. This central octahedron is connected through the vertices

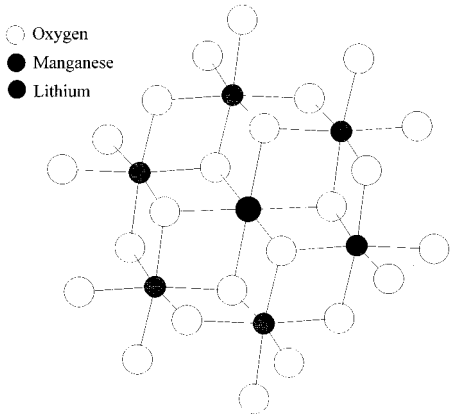

FIG. 3. Spatial arrangement of the Mn^{4+} ions surrounding the Li1 site.

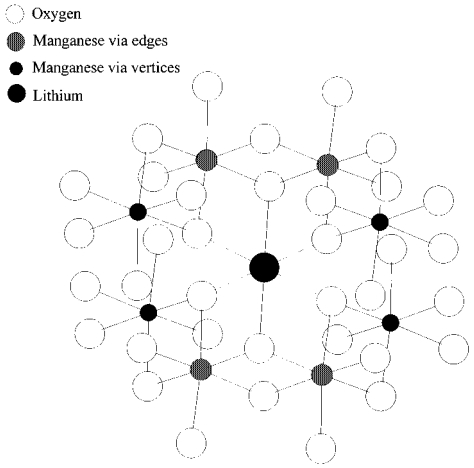

FIG. 4. Spatial arrangement of the Mn^{4+} ions surrounding the Li2 site.

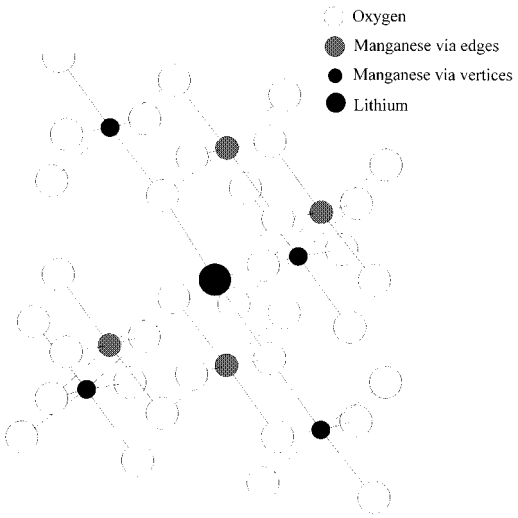

FIG. 5. Spatial arrangement of the Mn^{4+} ions surrounding the Li3 site.

with 6 octahedra, 4 of which with Mn at the center (distances from Li3: 4.007 and 4.060 Å) and shares edges with 12 octahedra, 4 of which centered on Mn (distances from Li3: 2.875 and 2.909 Å). The average values are reported in Table I. Figure 5 shows the spatial arrangement of the eight Mn polyhedra surrounding the Li3 ion. It can be noted that a strict similarity exists concerning the neighborhood of Li2 and Li3 sites. However, greater Li-Mn distances can be observed between Li3 and the Mn of the octahedra sharing the edges.

The three lithium sites are distinguishable for what concerns the shell of nearest-neighbor Mn^{4+} ions and the respective distances Li-Mn, and can likely undergo three different levels of hyperfine interaction with observable effects in NMR spectra.

Similar considerations can be also done when the Li_2MnO_3 phase coexists with the spinel ones ($x=0.40$): in this case the distances Li-Mn for the three lithium sites are altogether more extended than that found in the pure Li_2MnO_3, in agreement with the cell volume expansion observed for decreasing x, as shown in Fig. 2(c).

B. The NMR information

1. Sample $x=0.333$ ($LiMn_2O_4$)

Figure 6 shows both static and MAS spectra for the spinel $LiMn_2O_4$. The static spectrum is Gaussian in nature. MAS rotation removes part of the electron-nucleus anisotropic interactions and gives origin to a manifold centered at ~450 ppm. In agreement with the crystallographic data, we found only one isotropic peak at 664 ppm. We attribute the Gaussian shape of the manifold to susceptibility broadening not completely removed by MAS.[11,30]

Our isotropic datum is not in agreement with the value (520 ppm) reported by Morgan *et al.*[22] On the other hand, they noted that an increase in MAS speed resulted in the isotropic shift moving towards higher field, and attributed this fact to a temperature effect. Their observation may be more simply explained by supposing an incorrect determination of the isotropic value. An upfield sideband, in fact, will

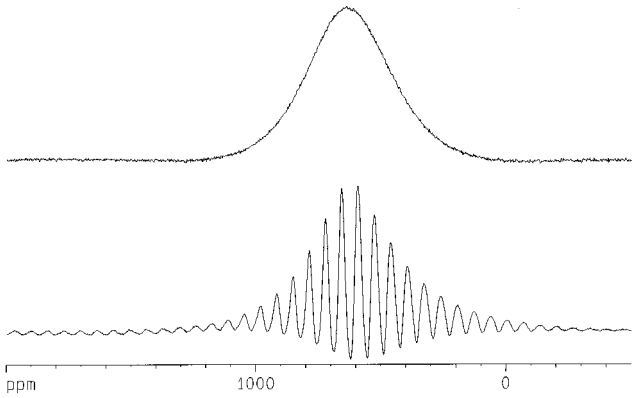

FIG. 6. Static (upper part) and MAS (lower part) ^{7}Li NMR spectra of sample $x=0.333$.

be further shifted towards high field by an increase of the rotation speed.

The stoichiometric spinel contains the same quantity of Mn^{3+} and Mn^{4+}. At room temperature, and for a magnetic field of 9.4 T, we obtain from Eq. (9) a value $\langle S_z\rangle=0.575$. The TFHI constant, in units of h, is $A=0.38\times10^{-4}$ cm^{-1}. This value refers, at a first approximation, to the manganese ions belonging to the first shell around each equivalent lithium ion, from which they are separated by two bonds. The contribution of outer manganese atoms may be neglected. In fact, Beshah *et al.* showed that in a magnetically diluted system the contribution of manganese ions belonging to the second shell (four bonds away) is tenfold reduced.[31]

In a paramagnetic system at room temperature it is reasonable to think that each manganese ion interacts independently with Li^+. Consequently, the hyperfine interaction is additive and it is possible to assign a ''mean shift'' of ~56 ppm to each manganese ion. Some NMR quantities are reported in Table I.

2. Sample $x=0.667$ (Li_2MnO_3)

As previously stated Li_2MnO_3 contains three nonequivalent lithium sites, one of which has multiplicity four and the others multiplicity two. Figure 7 shows both static and MAS spectra for this sample. Three isotropic peaks are found at 850, 875, and 1770 ppm, respectively. These values are in

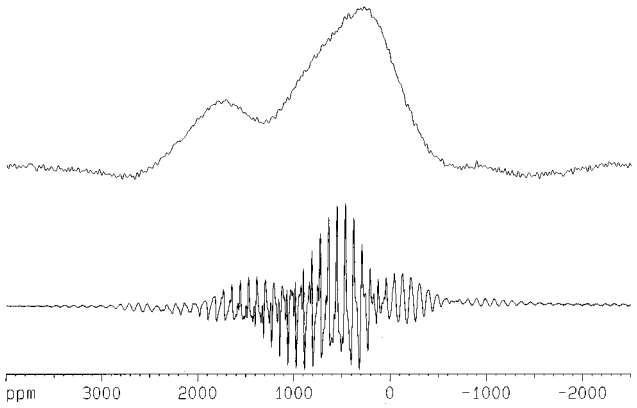

FIG. 7. Static (upper part) and MAS (lower part) ^{7}Li NMR spectra of sample $x=0.667$.

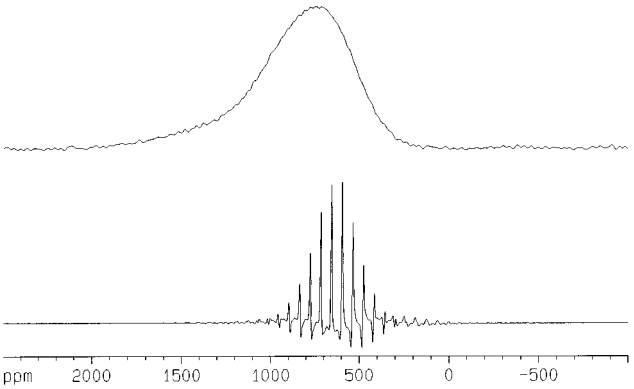

FIG. 8. Static (upper part) and MAS (lower part) ^{7}Li NMR spectra of sample $x=0.40$.

good agreement with the data reported in Ref. 22, except for a systematic difference of 50 ppm, which is the chemical shift of LiCl in our magnet for a carrier frequency of 155.6 MHz.

The peaks assignment is quite straightforward. In fact, Li2 and Li3 have the same number of manganese atoms nearly at the same average distance (see Table I). Then, the two near peaks in the range 850–900 ppm may be assigned to Li2 and Li3. The higher multiplicity of Li3 allows to assign the peak at 850 ppm to this moiety and the one at 875 ppm to Li2. The peak at 1770 ppm is assigned to Li1. We stress that it is not possible to obtain full quantitative information from a manifold of several thousands ppm because of the distortions related to the spectral width of the rf pulse.

Some information about the dominant term in the hyperfine interaction may be obtained by examining the relationships between the chemical shifts and Li-Mn distances. Because of the additivity of the interaction each manganese which surrounds a Li1 contributes a shift of about 295 ppm. Both Li2 and Li3 have in their first shell four Mn at less than 3 Å, and four at ~4 Å. Let us neglect the latter. If we hypothesize the dipolar interaction to be the dominant one, that is

$$\Delta\omega \propto \frac{K}{r^3}, \tag{11}$$

we will obtain theoretical shifts of 1125 ppm for Li2 and 1119 ppm for Li3, which demonstrates that the main contribution comes for Fermi contact. We may suppose that the major parameters affecting the interaction are covalency, hybridization, and angle bonds, in a similar fashion to that proposed by Spalek *et al.* to interpret the magnetic properties of diluted semiconductors.[32]

3. Sample x =0.40

The sample $x=0.40$ contains both the two spinel phases and the rocksalt compound. X-ray Rietveld refinement gives about 10% of Li_2MnO_3, whereas the remaining 90% contains phases I and II in the same amount. NMR shows a big peak at 658 ppm due to the spinel phase(s), and the three peaks of the rocksalt phase which are downshifted at 787, 838, and 1600 ppm, respectively (see Fig. 8). A small peak (2–3%) is found at ~0 ppm, that is likely due to unreacted Li_2CO_3.[22] The diamagnetic shift of the rocksalt peaks is simply accounted for by considering that the unit-cell volume increases when passing from $x=0.667$ to 0.4, as shown in Fig. 2(c). Again, the Fermi contact should be the dominant factor. In fact, by fitting our data with expression (11), we obtain a value ~41 for the exponent.

We were not able to find a peak that could be surely attributed to the substitutional lithium of spinel phase II. The reason can be that this population is magnetically equivalent to one of those belonging to the rocksalt structure, or that a lowering of the symmetry (not observed in our sample) introduces additional broadenings related to quadrupolar interaction. Itoh *et al.*[33] invoked the latter explanation to justify the decrease of static NMR intensity vs y in the nonstoichiometric spinel $Li_{1+y}Ti_{2-y}O_4$. However, their conclusions have been strongly criticized.[18]

Some interesting questions arise about the multiplicity and the chemical shift of the peak attributed to the spinel phases. Since the tetrahedral Li ions belonging to phases I and II are not magnetically equivalent, we would expect to have two distinct NMR peaks with approximately the same areas. The presence of a single feature can be accounted for by invoking one of the following reasons: (i) the two peaks have very similar chemical shifts, or (ii) a motional narrowing mechanism is acting (lithium ions that hop between the two phases), which is characterized by a correlation time shorter than the inverse of the peaks angular frequency difference, $\Delta\omega_{\mathrm{I,II}}$.

The former possibility can be ruled out because the peak is shifted upfield with respect to that of the $x=0.333$ one, whereas we see from Table I that the average Li-Mn distance of the stoichiometric phase decreases from $x=0.333$ to 0.40, which should mean a stronger hyperfine interaction.

Phase II displays even shorter Li-Mn distances. However, it has a ~10% excess of Li ions that occupy octahedral positions. The overall shift of the related NMR peak is likely to be the sum of two competing effects: a paramagnetic one related to cell contraction, and a diamagnetic one due to the decrease of the average number of manganese ions which surround each tetrahedral lithium

$$\Delta\omega_{\mathrm{tot,II}} = \Delta\omega_{\mathrm{dia,II}} + \Delta\omega_{\mathrm{par,II}}. \tag{12}$$

Since the populations of the two phases are nearly numerically equivalent, as shown by XRD, motional narrowing can give a single upfield peak only if the peak of phase II is shifted upfield more than the one of phase I is shifted downfield. This requires the diamagnetic term in Eq. (12) to be the predominant one. Under these assumptions, only one peak will be observed, with isotropic shift intermediate between the ones of phases I and II. Due to the populations equivalence, the upfield shift (~6 ppm) of the spinel peak in the sample $x=0.40$ allows us to estimate a minimum value $\Delta\omega_{\mathrm{I,II}} \cong 12$ ppm.

We cannot simply evaluate the two addenda of Eq. (12). In particular, Fermi contact is the predominant contribution to $\Delta\omega_{\mathrm{par,II}}$. However, a motional narrowing mechanism works if the following relationship holds

$$l < \sqrt{\frac{D}{\Delta\omega_{\mathrm{I,II}}}}, \tag{13}$$

where D is the lithium self-diffusion coefficient, and l is the linear dimension of the regions over which the motional process occurs. In our previous work[4] we found for phase II a linear dimension, l, of the order of 100 Å. Under the assumptions we made about $\Delta\omega_{I,II}$ we obtain for the self-diffusion coefficient a value of the order of 10^{-8} cm^2 s^{-1}, in agreement with the findings of Saïdi *et al.*[34]

V. CONCLUSIONS

The present results point out that the transferred hyperfine coupling between Mn ions and Li spins is the interaction dominating the NMR signal. From MAS spectra the pertinent parameters have been obtained in nondiluted Mn-Li oxides.

The spectral assignments for all the samples agree with our structural data, reporting the number of nonequivalent cation sites, the coordination type, and the distances (see Table I).

We stress that our conclusions about the motional narrowing process between the two spinel phases in the sample $x=0.40$ are just based on an assumption, although very reasonable. We cannot fully exclude, for example, that the spinel cell contraction from $x=0.33$ to 0.40 may cause a sign change of the TFHI constant. Since the Li^+ mobility is temperature activated, NMR measurements performed at low temperature could confirm our hypotheses. These experiments are in preparation.

ACKNOWLEDGMENTS

This work was partially funded by CSGI. NMR measurements have been performed at Centro Grandi Strumenti of the University of Pavia, with the help of Dr. Francesca Benevelli.

[1] P. Barboux, J. M. Tarascon, and F. K. Shokohi, J. Solid State Chem. **94**, 185 (1991).
[2] G. Pistoia, G. Wang, and C. Wang, Solid State Ion. **58**, 285 (1992).
[3] G. A. Martin, A. Bates, V. Ducarme, and C. Mirodates, Appl. Catal. **47**, 289 (1989).
[4] V. Massarotti, M. Bini, and D. Capsoni, Z. Naturforsch. Teil A **51**, 267 (1996).
[5] V. Massarotti, D. Capsoni, M. Bini, C. B. Azzoni, and A. Paleari, J. Solid State Chem. (to be published).
[6] P. Strobel and B. Lambert-Andron, J. Solid State Chem. **75**, 90 (1988).
[7] D. G. Wickham and W. J. Croft, J. Phys. Chem. Solids **7**, 351 (1958).
[8] J. M. Mays, Phys. Rev. **131**, 38 (1963).
[9] R. G. Shulman and V. Jaccarino, Phys. Rev. **108**, 1219 (1957).
[10] R. G. Shulman and K. Knox, Phys. Rev. **119**, 94 (1960).
[11] M. E. Stoll and T. J. Majors, Phys. Rev. B **24**, 2859 (1981).
[12] W. P. Rothwell, J. S. Waugh, and J. P. Yesinowski, J. Am. Chem. Soc. **102**, 2637 (1980).
[13] E. T. Olejniczak, S. Vega, and R. G. Griffin, J. Chem. Phys. **81**, 4804 (1984).
[14] A. Nayeem and J. P. Yesinowski, J. Chem. Phys. **89**, 4600 (1988).
[15] A. K. Cheetham, C. M. Dobson, C. P. Grey, and R. J. B. Jakeman, Nature **328**, 706 (1987).
[16] C. P. Grey, C. M. Dobson, A. K. Cheetham, and R. J. B. Jakeman, J. Am. Chem. Soc. **111**, 505 (1989).
[17] M. Dalton, D. P. Tunstall, J. Todd, S. Arumugam, and P. P. Edwards, J. Phys. Condens. Matter **6**, 8859 (1994).
[18] P. Ganguly, V. Ramaswamy, I. S. Mulla, R. F. Shinde, P. P. Bakare, S. Ganapathy, P. R. Rajamohanan, and N. V. K. Prakash, Phys. Rev. B **46**, 11 595 (1992).
[19] C. Marichal, J. Hirschinger, P. Granger, M. Menetrier, A. Rougier, and C. Delmas, Inorg. Chem. **34**, 1773 (1995).
[20] Y. Kanzaki, A. Taniguchi, and M. Abe, J. Electrochem. Soc. **138**, 334 (1991).
[21] N. Kumagai, T. Fujiwara, and K. Tanno, J. Electrochem. Soc. **143**, 1007 (1996).
[22] K. R. Morgan, S. Collier, G. Burns, and K. Ooi, J. Chem. Soc., Chem. Commun. **2**, 1719 (1994).
[23] C. Masquelier, M. Tabuchi, K. Ado, R. Kanno, Y. Kobayashi, Y. Maki, O. Nakamura, and J. B. Goodenough, J. Solid State Chem. **123**, 255 (1996).
[24] H. M. Rietveld, J. Appl. Cryst. **2**, 65 (1969).
[25] D. B. Wiles and R. A. Young, J. Appl. Cryst. **14**, 149 (1981).
[26] J. Schneider, Acta Crystallogr. A **43**, C295 (1987).
[27] V. Massarotti, D. Capsoni, and M. Bini, Z. Naturforsch. Teil A 50, 155 (1995).
[28] M. Bose, in *Progress in Nuclear Magnetic Resonance Spectroscopy*, edited by J. W. Emsley, J. Feeney, and L. H. Sutcliffe (Pergamon, London, 1969), Vol. 4, pp. 335–444.
[29] H. M. McConnell and R. E. Robertson, J. Chem. Phys. **29**, 1361 (1958).
[30] C. P. Grey, C. M. Dobson, and A. K. Cheetham, J. Magn. Reson. **98**, 414 (1992).
[31] K. Beshah, P. Becla, R. G. Griffin, and D. Zamir, Phys. Rev. B **48**, 2183 (1993).
[32] J. Spalek, A. Lewicki, Z. Tarnawski, J. K. Furdyna, R. R. Galazka, and Z. Obszko, Phys. Rev. B **33**, 3407 (1986).
[33] M. Itoh, Y. Hasegawa, H. Yasuoka, Y. Ueda, and K. Kosuge, Physica C **157**, 65 (1989).
[34] M. Y. Saïdi, J. Barker, and R. Koksbang, J. Solid State Chem. **122**, 195 (1996).